Supporting Information for "Joint inversion of satellite-detected tidal and magnetospheric signals constrains electrical conductivity and water content of the upper mantle and transition zone"

A. V. Grayver[1], F. D. Munch[1], A. V. Kuvshinov[1], A. Khan[1], T. J. Sabaka[2],

L. Tøffner-Clausen[3]

Contents of this file

1. Caption to figures S1 to S4

Introduction

Corresponding author: A. V. Grayver, Institute of Geophysics, ETH Zürich, Sonneggstrasse 5, 8092 Zurich, Switzerland. (agrayver@erdw.ethz.ch)

[1]Institute of Geophysics, ETH Zürich,

Switzerland.

[2]Planetary Geodynamics Laboratory,

NASA/GSFC, USA

[3]DTU Space, Technical University of

Denmark, Denmark

In the main paper, we showed inversion results using real satellite data. To gain more insight into how the different methods/data contribute to the recovered models, we ran a number of inversions based on a synthetic model (Figure S1). Corresponding responses for the recovered profiles are shown in Figure S2. These results serve to emphasize where the various data sets have their main sensitivity. For example, Figure S1a shows that inversion of C-responses only is not capable of resolving upper mantle conductivity structure, whereas inversion of tidally-induced signals (Figure S1b) has strong sensitivity to the lithosphere-asthenosphere boundary but can not constrain the conductivity structure of the transition zone and lower mantle. Only with a joint inversion of both data sets (Figure S1c) is it possible to constrain the entire mantle. Note that in Figure S2, C_1-responses computed based on model M2 only do not fit the synthetic data. This results directly from the fact that M2 is not required to fit the C_1-responses, but only the tidal magnetic signals.

Additionally, we compared laboratory-based conductivity profiles with the conductivity profiles obtained from inversion of satellite magnetic data. The laboratory-based conductivity profile is derived from the application of self-consistent thermodynamic phase equilibrium computations that are based on free-energy minimization. The corresponding phase diagram is shown in Figure S3. To further demonstrate the consistency of our results, we computed radial seismic P- and S-wave speeds and density for the same composition and geotherm described in the main paper and compare the resulting profiles with the Preliminary Reference Earth Model (PREM) in Figure S4. Apart from the 220-km seismic discontinuity, which is a PREM-only feature, the agreement is excellent.

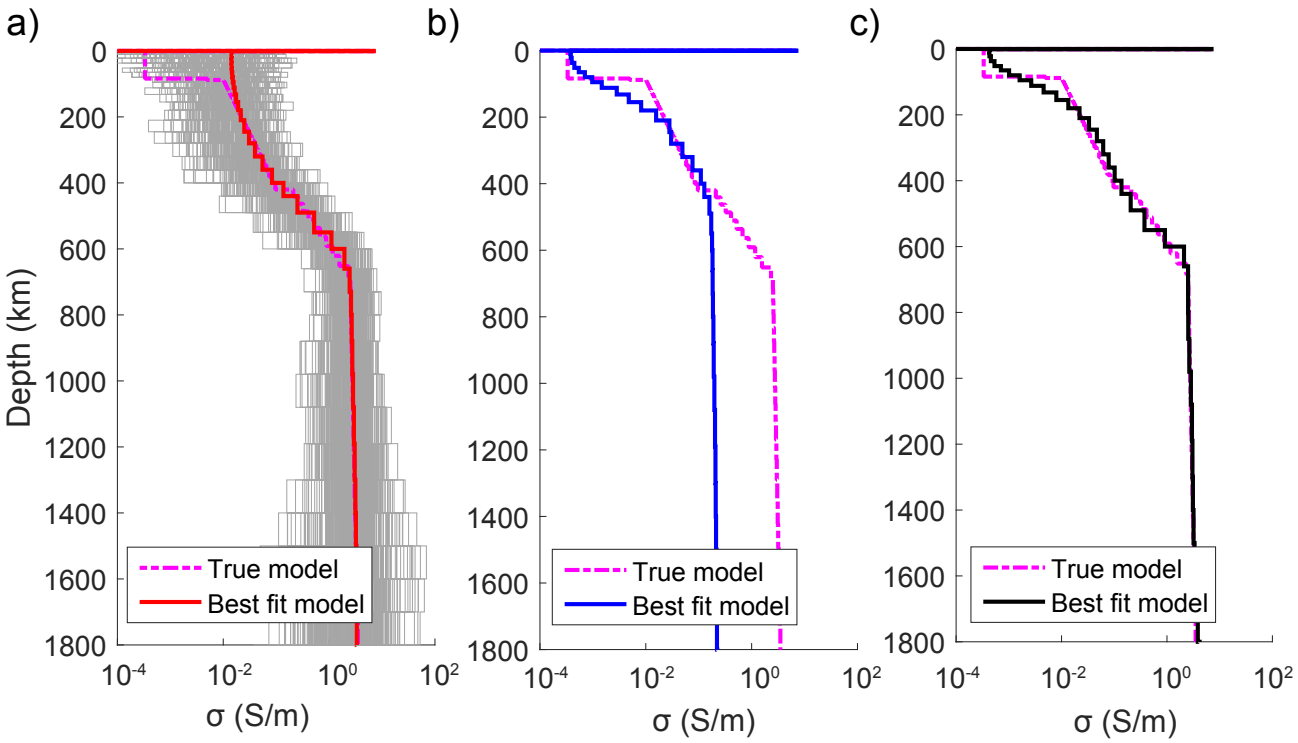

Figure S1. Conductivity models derived from inverting synthetic profile ("True model") using only C_1-responses (a), tidal magnetic signals (b) and both simultaneously (c). For the inversion of C-responses only (a), we also performed MCMC sampling. The results (shown as gray lines) emphasize that C-responses are not sensitive to upper mantle conductivity structure.

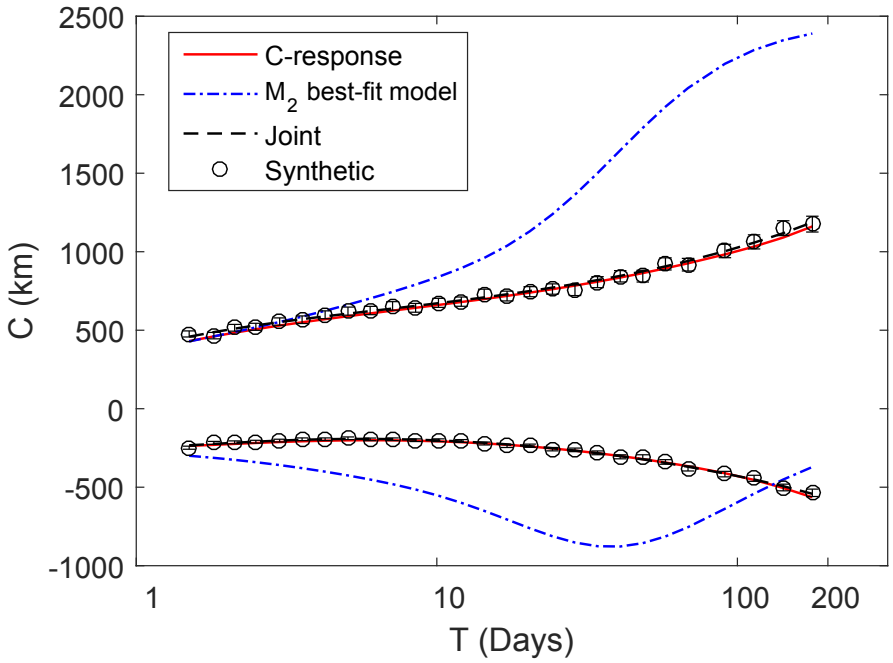

Figure S2. C_1-responses calculated for the models shown in Figure S1. Synthetic responses were contaminated with 3% random Gaussian noise.

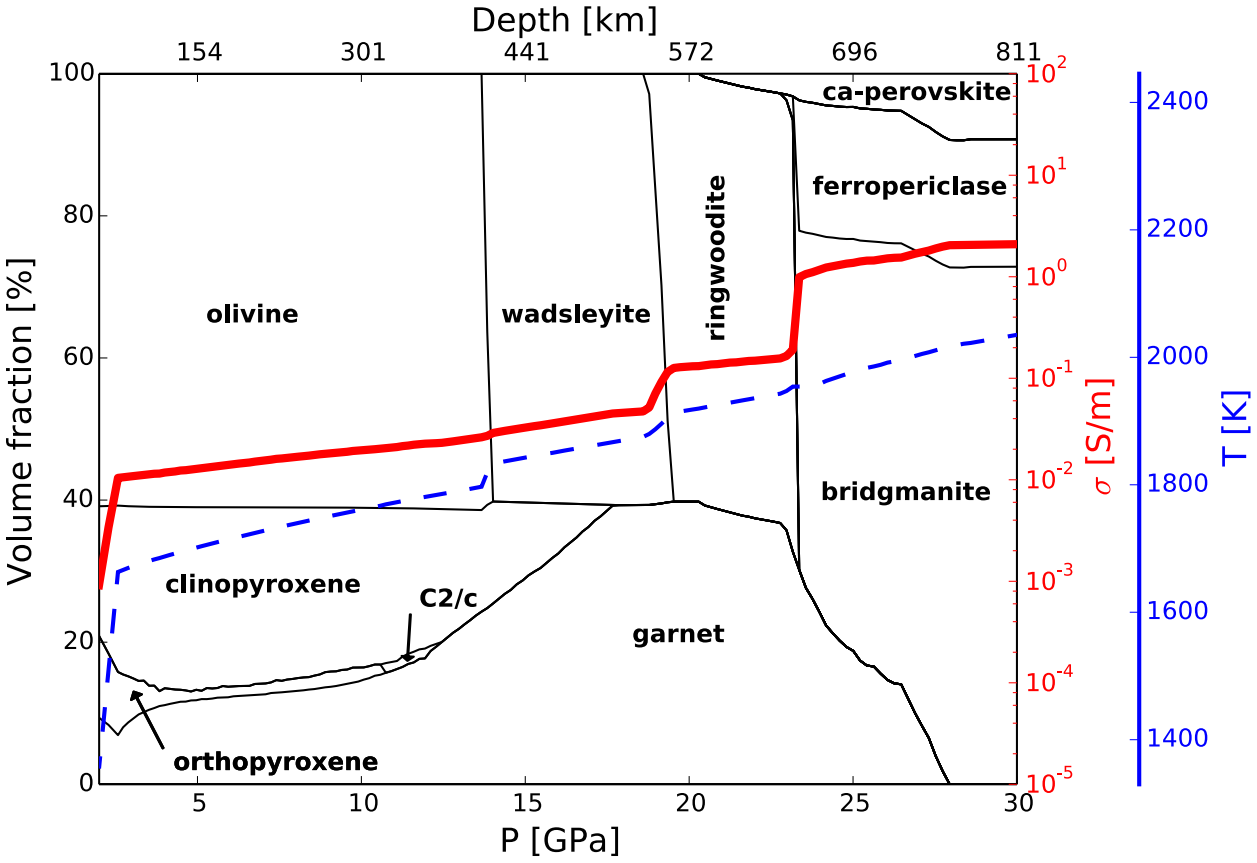

Figure S3. Variations in phase proportions for a pyrolitic mantle based on self-consistent thermodynamic calculations. Dashed blue line shows a calculated thermal profile. Solid red line shows the bulk electrical conductivity profile in the case of a dry mantle.

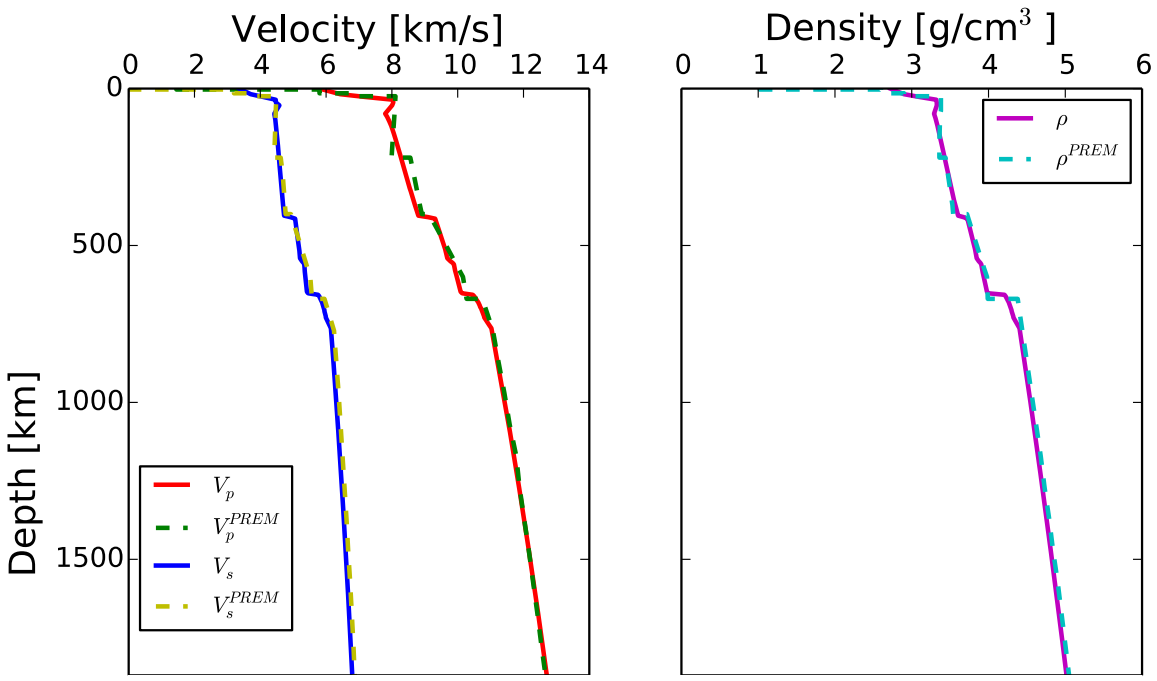

Figure S4. Comparison of computed seismic P- and S-wave speeds and density with Preliminary Reference Earth Model (PREM). The computed properties shown here are based on the same composition and geotherm (see Figure S3) as those used to compute the laboratory-based conductivity profile (shown in Figure 6) of the main paper.